MEAN TEMPERATURE MODEL FOR INCOMPRESSIBLE WALL-BOUNDED TURBULENCE OVER A WIDE RANGE OF PRANDTL NUMBERS

Justin E. Ka Ip Sun
Department of Mechanical and Aerospace Engineering
The Hong Kong University of Science and Technology
Clear Water Bay, Kowloon, Hong Kong
kijesun@connect.ust.hk

Lin Fu[1]
Department of Mechanical and Aerospace Engineering
Department of Mathematics
The Hong Kong University of Science and Technology
Clear Water Bay, Kowloon, Hong Kong
linfu@ust.hk

ABSTRACT

A model of the mean temperature profile which considers variations in fluid medium and therefore the Prandtl number (Pr) is proposed within incompressible wall-bounded turbulence. The model is based on a novel relationship between momentum and thermal eddy diffusivity for a wide range of Pr ($0.007 \leq Pr \leq 10$) and Re_τ ($179 \lesssim Re_\tau \lesssim 5000$) in both incompressible channel and boundary layer flows. It exhibits improved overall average accuracy compared to existing models, since it can better capture the thermal profile behaviours at low Pr. Across all cases, the proposed framework reduces the average error compared to existing methods, showcasing a new temperature-velocity (TV) relationship which accounts for large variations in Pr.

INTRODUCTION

Turbulent flows play a crucial role in the transport of thermal energy and physical matter within fluid flows since their chaotic motions promote enhanced interlayer mixing compared to laminar flow, where the differences in their thermal or matter transport can be encapsulated within the molecular Prandtl number ($Pr = \nu/\alpha$), the ratio between kinematic viscosity (ν) and the thermal diffusivity (α), and the Schmidt number ($Sc = \nu/D$), the ratio between the kinematic viscosity and the mass diffusivity (D). Physical understanding of flows with heat transfer or mass transport at Pr, $Sc \approx 1$ is obvious since the velocity behaviour will be identical to the temperature or contaminant behaviours, but in reality, different flow mediums exhibit a wide range of Pr and Sc. Commonplace fluids in engineering, such as water, engine oils, glycerol, and polymer melts, have significantly higher Pr than 1, whereas low and very low Pr flows are important in the simulation of nuclear liquid metal reactors (LMR) and concentrated solar power (CSP) technologies. In practice, Sc is also typically much greater than 1 for the diffusion of contaminants.

Furthermore, despite the proposed thermal law of the wall, its parameter variations exhibit strong Pr dependence, where the logarithmic region is not readily present at lower Pr (Alcántara-Ávila *et al.*, 2018). Therefore, the relationship between momentum transfer and heat transfer has always received considerable attention, particularly, how to relate the mean streamwise velocity and temperature profiles.

Our focus in the following will be on heat transfer, but note that the study and its discussions hereafter could also be applied to the diffusion of contaminants by replacing Pr with Sc and other thermal-related quantities with mass-diffusivity equivalents.

EXISTING METHODOLOGIES

Johnson-King (JK) Model

The JK model (Johnson & King, 1985) is an empirical model, originally for the momentum eddy diffusivity, adapted by Pirozzoli (2023*b*) to capture the variations in the thermal eddy diffusivity, α_t^+:

$$\alpha_t^+ = \frac{-\overline{v'^+\Theta'^+}}{\dfrac{d\Theta^+}{dy^+}} \tag{1}$$

where $\Theta = T_w - T$, which is the difference between the wall temperature, indicated by the subscript $_w$, and the mean temperature at a wall-normal position, T. v is the wall-normal velocity, the superscript $^+$ denotes viscous scaling, the overbar $\overline{(\cdot)}$ denotes Reynolds averaging, and $'$ denotes the fluctuations from Reynolds averaging. They modelled the thermal eddy diffusivity via a damping function:

$$\alpha_{t,\mathrm{JK}}^+ = \kappa_t y^+ \left[1 - \exp\left(-\frac{y^+}{A_\theta}\right)\right]^2 \tag{2}$$

[1]Corresponding author.

where $A_\theta = 19.2$ and the thermal von Kármán constant $\kappa_t = 0.459$. A closure model is found using the a known expression of the total heat flux q^+ to find the temperature gradient (see Eq. (10) later). However, it has large overestimations in the outer region, and κ_t has exhibited large variations with respect to Pr, leading to weaker universality for the model.

Explicit Scalar Mean Profile for Internal Flows

Also focusing on the inner-layer, Pirozzoli (2023*a*) derived an explicit formula for the mean profiles of passive scalars in pipe flows for a wide range of Prandtl numbers ($0.00625 \leq Pr \leq 16$). Based on an expression of the momentum eddy viscosity by Musker (1979), a functional form of the thermal eddy diffusivity can be written as follows:

$$\alpha^+_{t,\mathrm{P}} = \frac{(\kappa_t y^+)^3}{(\kappa_t y^+)^2 + C_\theta^2} \tag{3}$$

where C_θ has been found to be 10 (Pirozzoli, 2023*a*). A direct integration of the temperature gradient via Eq. (3) yields an explicit expression for the mean temperature profile, denoted as Θ^+_P, as the Pirozzoli (P) model. We refer the readers to the original study by Pirozzoli (2023*a*) since the full formula is too long and complex to be included here. This resulted in improved accuracy compared to the JK model, but some deviations from DNS in the outer layers and at the lowest Pr ($Pr \lesssim 0.125$) still remain.

Incorporation of Outer Layer Modelling

To better capture the outer-layer mean temperature profile, Pirozzoli & Modesti (2024) further combined Θ^+_P with an analytical form for the wake (outer) region of the flow, where, upon investigation of the temperature defect profile found outer-layer universality for $Pr \gtrsim 0.025$ (Pirozzoli *et al.*, 2016, 2021, 2022). Using a constant thermal eddy diffusivity assumption, the following form of the outer layer temperature can be derived

$$\Theta^+_e - \Theta^+_c = C_w \left(1 - \frac{y}{h}\right)^2 \tag{4}$$

where Θ^+_c is the desired mean temperature profile (core mean temperature profile), Θ^+_e is the mean temperature at the boundary layer edge, and C_w is a parameter depending on the flow type and wall conditions (Pirozzoli & Modesti, 2024). A final explicit model for the entire mean temperature profile is obtained by combining the inner-layer model (Pirozzoli, 2023*a*) and the outer-layer model Eq. (4). A smooth patching point through the continuity of the temperature gradient is found at

$$\frac{y^*}{h} = \frac{1}{2}\left(1 - \sqrt{1 - \frac{2}{C_w \kappa_t}}\right) \tag{5}$$

implying

$$\Theta^+_e = \Theta^+_\mathrm{P}(y^{*+}, Pr) + C_w \left(1 - \frac{y^*}{h}\right)^2 \tag{6}$$

We again refer the readers to the original paper by Pirozzoli & Modesti (2024) due to the complexity of the final model expression.

Current Areas to Tackle

The PM model presents a very accurate prediction of the mean temperature profiles for internal flows, i.e., pipes and channels, where parameters can be adjusted for boundary conditions such as asymmetric heating. However, noticeable deviations still exist at the smaller Pr since the basis of the PM model relies on the existence of a logarithmic layer, whereas low Pr flows lack this distinctive region at low to moderate Re_τ. Since the reviewed models all have poorer performance at the lower Prandtl number flows, where these small temperature differences are critical in practice, one of our major focuses will be on capturing the dynamics of low-Pr mean temperature profiles. Another canonical wall-bounded flow type to consider is turbulent boundary layers. Outer-layer universality, Eq. (4) holds only for internal flows, and turbulent boundary layers were not considered in detail in previous studies. Therefore, we look to investigate the models in boundary layer flows as well. Lastly, explicit relationships between temperature and velocity quantities are often desired since they may be able to provide further insight into the similarities and dynamics of thermal and momentum statistics of turbulence, in a Reynolds-analogy-like manner.

DATA

The DNS data used in this study are a set of incompressible turbulent channel (Alcántara-Ávila *et al.*, 2018; Alcántara-Ávila & Hoyas, 2021; Alcántara-Ávila *et al.*, 2021) and boundary layer (Balasubramanian *et al.*, 2023) flows, with flow parameters shown in table 1.

Table 1. Basic flow parameters of the DNS data used.

Configuration	Re_τ	Pr
Channel	500-5000	0.007 - 10
Boundary Layer	179 - 403	1 - 6

PROPOSED METHODOLOGY

We propose a new relationship bewteen α^+_t and the momentum eddy diffusvity, ν^+_t, which is defined as follows:

$$\nu^+_t = \frac{-\overline{u'^+ v'^+}}{\dfrac{du^+}{dy^+}} \tag{7}$$

Through figure 1, we can see that ν^+_t and α^+_t display similarities at the same Pr across different Re_τ. This gives us some inspiration to capture the relationship between them, using a very simple linear form as follows:

$$\widehat{\left(\frac{\alpha^+_t}{\nu^+_t}\right)}_{\text{est.}} = \hat{m}\left(\frac{y}{h}\right) + \hat{c} \tag{8}$$

To obtain the parameters $\hat{m}$ and $\hat{c}$, we first perform a case-by-case optimisation to find the linear line of best fit, where

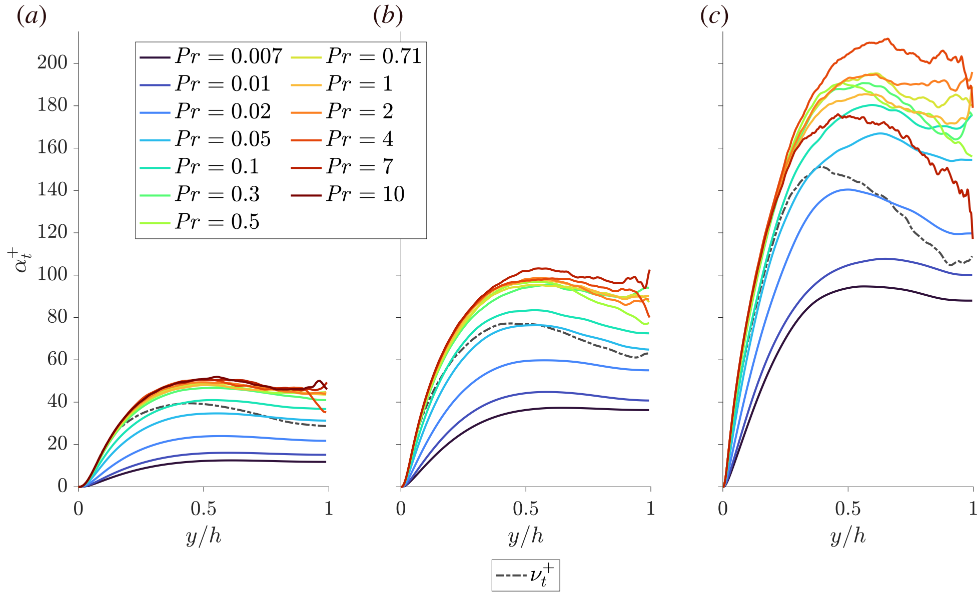

Figure 1. Wall-normal profiles of the momentum eddy diffusivity, ν_t^+, and the thermal eddy diffusivity, α_t^+, for: (*a*) $Re_\tau \approx 500$, (*b*) $Re_\tau \approx 1000$, and (*c*) $Re_\tau \approx 2000$, at different Pr respectively.

we can find the gradient m and intercept c. These optimised coefficients are shown in figure 2, where they are plotted with respect to Re and Pr. While no observable trends are seen with respect to Re_τ, c shows a clear trend, where it is captured by the following fit:

$$\hat{c}(Pr) = 0.85677[1 - \exp(-22.0276Pr)] + 0.14512 \quad (9)$$

On the other hand, while m does show a weak trend at low Pr, it does not warrant a separate fit, such that an average value is taken to prevent overfitting and improve generalisation, where $\hat{m} = 0.4951$. We note the total heat flux has the following relation with α_t^+:

$$q^+ = \underbrace{k^+ \frac{d\Theta^+}{dy^+}}_{\text{Molecular}} \underbrace{- \overline{v'^+ \Theta'^+}}_{\text{Turbulent}} = \left(\frac{1}{Pr} + \alpha_t^+ \right) \frac{d\Theta^+}{dy^+} \quad (10)$$

where $k^+ = \dfrac{1}{Pr}$. With an empirical expression for the total heat flux available in an incompressible channel (Alcántara-Ávila *et al.*, 2018):

$$q^+ = 1 - \frac{1}{Re_\tau} \int_0^{y^+} \frac{u^+}{U_b^+} dy \quad (11)$$

where Re_τ is the friction Reynolds number, y is the wall-normal position, u is the streamwise velocity, and U_b is the bulk velocity, and combined with an empirically known total shear stress τ^+ in channel flows:

$$\tau^+ = \underbrace{\frac{1}{Re_\tau} \frac{du^+}{dy}}_{\text{Molecular}} \underbrace{- \overline{u'^+ v'^+}}_{\text{Turbulent}} = 1 - \frac{y}{h} \quad (12)$$

results in a closure model for the mean temperature based on velocity and related statistics only, as follows:

$$\widehat{\Theta}^+ = \int_0^{y^+} \frac{d\widehat{\Theta^+}}{dy^+} dy^+ = \int_0^{y^+} \frac{q^+}{\dfrac{1}{Pr} + \nu_t^+ \widehat{\left(\dfrac{\alpha_t^+}{\nu_t^+} \right)}_{\text{est.}}} dy^+ \quad (13)$$

However, in turbulent boundary layer flows, there is no closed expression for q^+ or τ^+, therefore, we borrow the estimation of the total shear stress from Chen *et al.* (2019):

$$\tau_{BL}^+ = 1 - \left(\frac{y}{\delta_{99}} \right)^{1.5} \quad (14)$$

where δ_{99} is the boundary layer thickness, and let $q^+ \approx \tau_{BL}^+$ to complete the closure model in turbulent boundary layers via an integration similar to Eq. (13) with the streamwise mean velocity profile as input to find ν_t^+.

RESULTS AND DISCUSSIONS

A representative selection of 9 channel flow cases are shown here for brevity, which are labelled as follows: $Re_\tau \approx 500$ and (*a*) $Pr = 0.007$, (*b*) $Pr = 0.3$, and (*c*) $Pr = 10$; at $Re_\tau \approx 1000$ and (*d*) $Pr = 0.01$, (*e*) $Pr = 0.5$, and (*f*) $Pr = 7$; and at $Re_\tau \approx 2000$ and (*g*) $Pr = 0.02$, (*h*) $Pr = 0.71$, and (*i*) $Pr = 4$. The subfigures of figures 3 and 4 are arranged such that Re_τ increases over each row, and Pr increases over each column. Their estimated thermal eddy diffusivities, $\hat{\alpha}_{t,\text{est.}}^+$, are shown in figure 3 compared to those from other methods and DNS. The current estimated $\hat{\alpha}_{t,\text{est.}}^+$ exhibits more accurate reconstructions, where other methods struggle in the outer layers and at low Pr. While the logarithmic ordinate (y-axis) under-represents the differences of other methods compared to DNS, the inset figures better show the scale differences. With improved modelling of α_t^+, we then show the final reconstructed mean temperature profiles in figure 4, where they show much

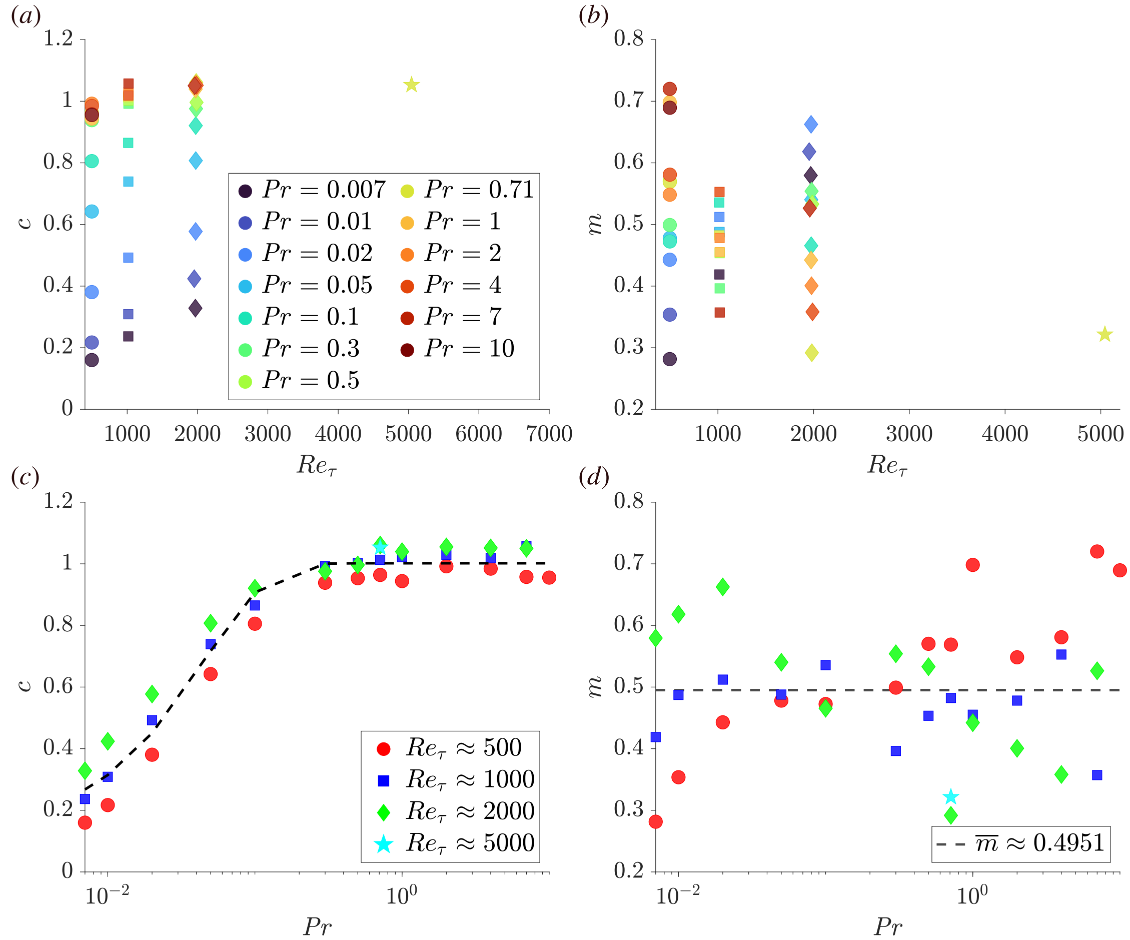

Figure 2. Thermal and momentum eddy diffusivities ratio linear estimator parameter variation with Re_τ and Pr. Subfigures (*a*-*b*) show the variation of c and m, respectively, against Re_τ, whereas subfigures (*c*-*d*) show the variation of c and m, respectively, against Pr. The black dashed line of best fit in subfigure (*c*) is shown in Eq. (9), whereas the black dashed line in subfigure (*d*) is the mean value of all m across the cases.

improved accuracy at low Pr, but as we move up in Pr, the improvements are lessened, and the current method performs slightly worse than existing methodologies. This is to be expected since we explicitly captured low-Pr behaviour only, and simply assumed relative universality of $\hat{m}$ and $\hat{c}$ at higher Pr. We note that the boundary layer cases exhibit similar performances at the same Pr for each model.

To quantify the results, we show the mean square errors (MSE) and mean absolute percentage errors (MAPE) in figure 5 and the average MAPE across all cases considered in table 2. While the JK model consistently performs worst across all cases, the current method shows improved accuracy at low Pr, and the PM model performs best at $Pr \geq 1$. However, on average, the current method still outperforms existing methods using a relatively simple linear model of Pr_t^{-1} as seen in table 2, capturing the distinctly different mechanisms at low Pr where strong conductive effects dominate (Abe & Antonia, 2009). These mechanisms led to a downward shift in α_t^+, which was then subsequently captured by the variation in $\hat{c}$, where it decreases at lower Pr.

Table 2. Average MAPE of different models across all the channel flow cases considered.

Model	Average MAPE
JK	14.37%
P	6.41%
PM	6.83%
Current	3.97%

ACKNOWLEDGEMENTS

This work was supported by the National Natural Science Foundation of China (No. 12422210). Justin E. Ka Ip Sun gratefully acknowledges the Hong Kong PhD Fellowship Scheme funded by the Research Grants Council (RGC) of the Hong Kong Special Administrative Region (HKSAR) Government (No. PF22-79233). Lin Fu also acknowledges the funding from the RGC of the HKSAR Government with RGC/ECS Project (No. 26200222), RGC/GRF Project (No. 16201023), RGC/STG Project (No. STG2/E-605/23-N) and RGC/TRS Project (No. T22-607/24N). Justin E. Ka Ip Sun would also like to extend his sincerest thanks to Dr. C. Cheng for their fruitful discussions.

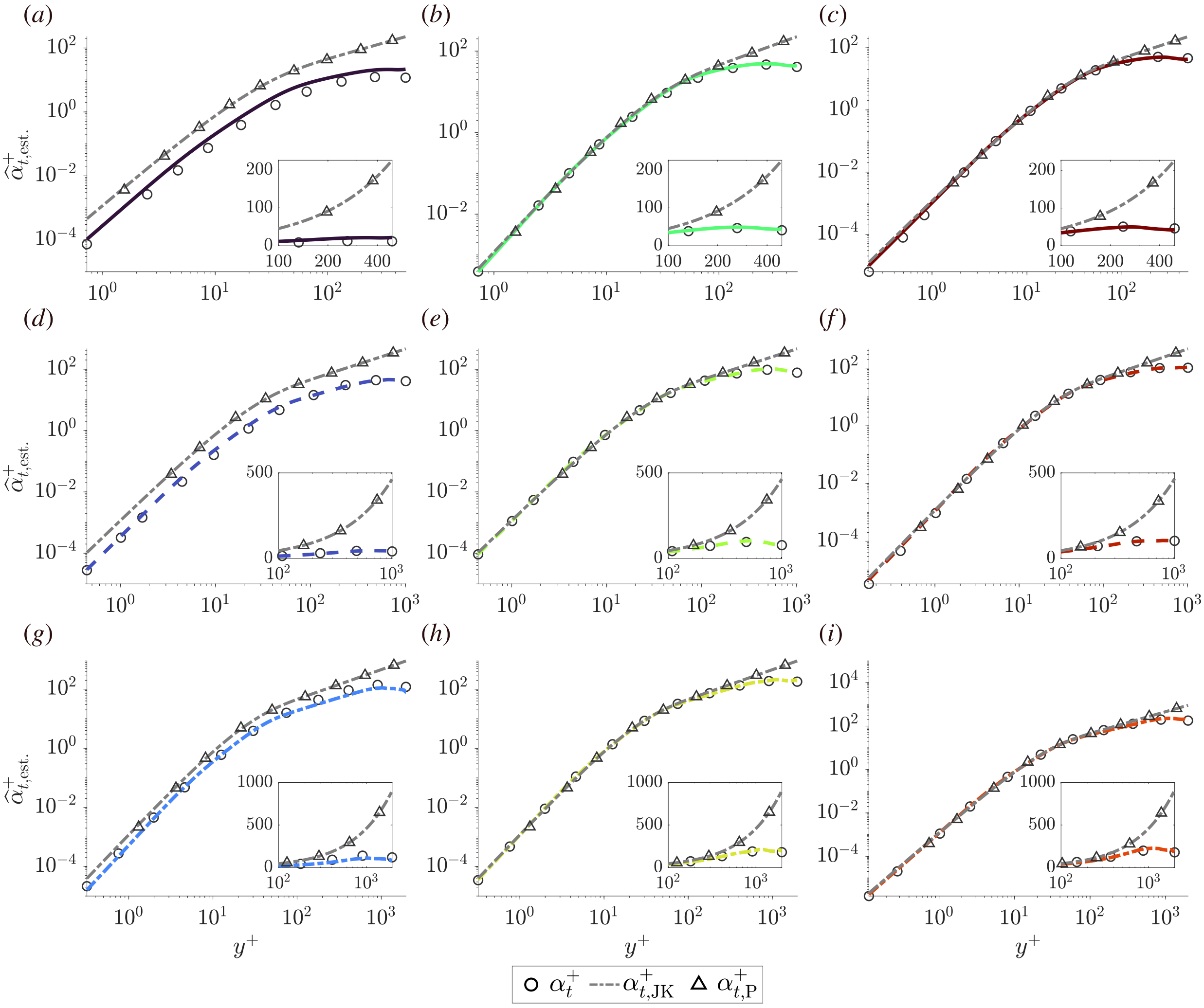

Figure 3. Proposed thermal eddy diffusivity model, $\widehat{\alpha}^+_{t,\mathrm{est.}}$, based on Eq. (8) assuming a known distribution of ν_t^+. They are compared to DNS, indicated by the unfilled circle markers, the JK model from Eq. (2), indicated by the dashed-dotted grey lines, and the P and PM model from Eq. (3), indicated by unfilled triangular markers. The ordinate (y-axis) is on a logarithmic scale. The inset figure is the same, except it is no longer on a logarithmic ordinate, to highlight the outer-layer deviations ($y^+ > 100$ shown here) from DNS.

REFERENCES

Abe, H. & Antonia, R. A. 2009 Turbulent Prandtl number in a channel flow for $Pr = 0.025$ and 0.71. In *Sixth International Symposium on Turbulence and Shear Flow Phenomena (TSFP6)*. Seoul, Korea.

Alcántara-Ávila, F. & Hoyas, S. 2021 Direct numerical simulation of thermal channel flow for medium–high Prandtl numbers up to $Re_\tau = 2000$. *Int. J. Heat Mass Transf.* **176**, 121412.

Alcántara-Ávila, F., Hoyas, S. & Pérez-Quiles, M. J. 2021 Direct Numerical Simulation of Thermal Channel Flow for $Re_\tau = 5000$ and $Pr = 0.71$. *J. Fluid Mech.* **916**, A29.

Alcántara-Ávila, F., Hoyas, S. & Pérez-Quiles, M. J. 2018 DNS of thermal channel flow up to $Re_\tau = 2000$ for medium to low Prandtl numbers. *Int. J. Heat Mass Transf.* **127**, 349–361.

Balasubramanian, A. G., Guastoni, L., Schlatter, P. & Vinuesa, R. 2023 Direct numerical simulation of a zero-pressure-gradient turbulent boundary layer with passive scalars up to Prandtl number $Pr = 6$. *J. Fluid Mech.* **974**, A49.

Chen, X., Hussain, F. & She, Z.-S. 2019 Non-universal scaling transition of momentum cascade in wall turbulence. *J. Fluid Mech.* **871**, R2.

Johnson, D. A. & King, L. S. 1985 A mathematically simple turbulence closure model for attached and separated turbulent boundary layers. *AIAA J.* **23** (11), 1684–1692.

Musker, A. J. 1979 Explicit Expression for the Smooth Wall Velocity Distribution in a Turbulent Boundary Layer. *AIAA J.* **17** (6), 655–657.

Pirozzoli, S. 2023*a* An explicit representation for mean profiles and fluxes in forced passive scalar convection. *J. Fluid Mech.* **968**, R1.

Pirozzoli, S. 2023*b* Prandtl number effects on passive scalars in turbulent pipe flow. *J. Fluid Mech.* **965**, A7.

Pirozzoli, S., Bernardini, M. & Orlandi, P. 2016 Passive scalars in turbulent channel flow at high reynolds number. *J. Fluid Mech.* **788**, 614–639.

Pirozzoli, S. & Modesti, D. 2024 Mean temperature profiles in turbulent internal flows. *Int. J. Heat Mass Transf.* **109**, 109544.

Pirozzoli, S., Romero, J., Fatica, M., Verzicco, R. & Orlandi, P. 2021 One-point statistics for turbulent pipe flow up to $Re_\tau \approx 6000$. *J. Fluid Mech.* **926**, A28.

Pirozzoli, S., Romero, J., Fatica, M., Verzicco, R. & Orlandi, P. 2022 DNS of passive scalars in turbulent pipe flow. *J. Fluid Mech.* **940**, A45.

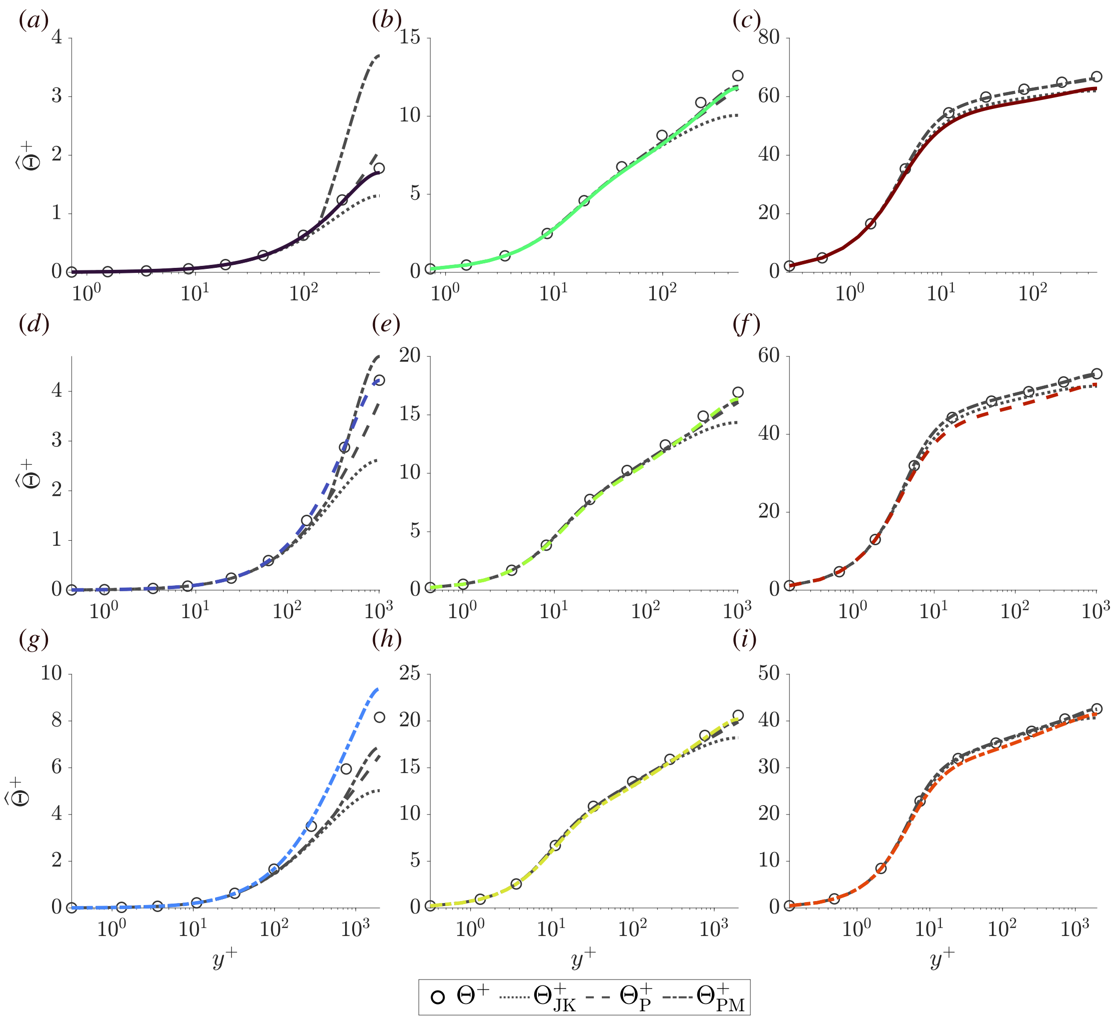

Figure 4. Comparisons of modelled mean temperature profiles between the currently proposed model compared to the JK model, the P model, the PM model, and DNS, represented by $\widehat{\Theta}^+$, Θ^+_{JK}, Θ^+_{P}, Θ^+_{PM}, and Θ^+, respectively.

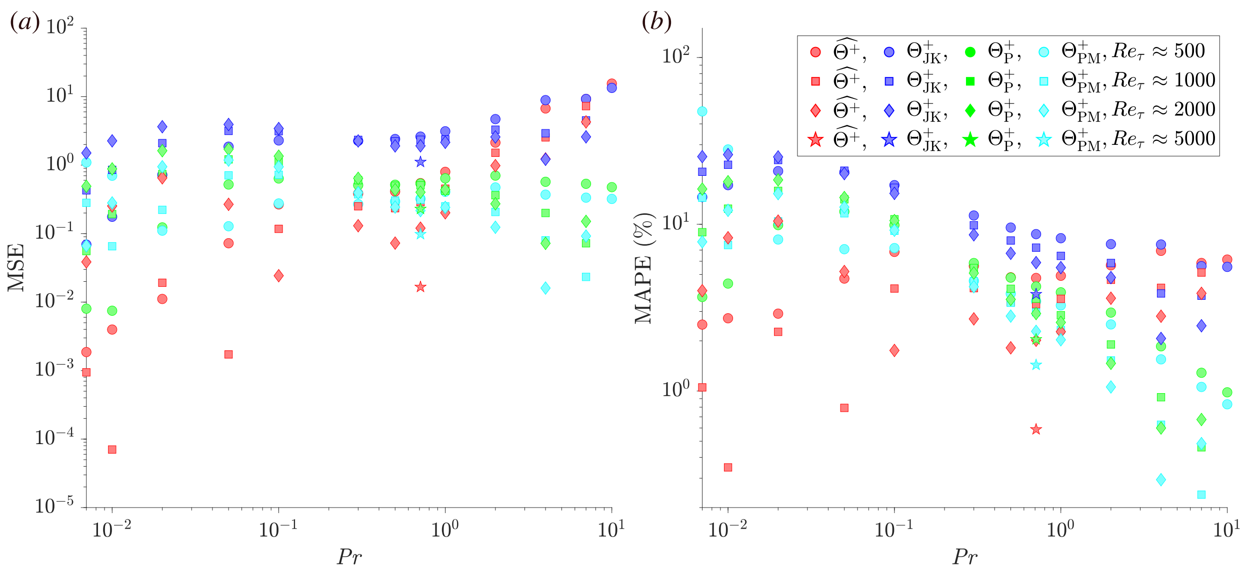

Figure 5. Errors of the currently proposed temperature model (red) compared to the JK model (blue), the P model (green), and the PM model (cyan). Errors are computed throughout the wall-normal profile against the mean temperature profiles from DNS. Subfigure (*a*) shows MSEs, while subfigure (*b*) displays the MAPEs.